

SPIN-DOWN MEASUREMENT OF PSR J1813–1749: THE ENERGETIC PULSAR POWERING
HESS J1813–178

J. P. HALPERN, E. V. GOTTHELF, AND F. CAMILO

Columbia Astrophysics Laboratory, Columbia University, 550 West 120th Street, New York, NY 10027-6601, USA

ABSTRACT

Two new X-ray timing observations of the 44.7 ms pulsar in G12.82–0.02/HESS J1813–178 were obtained with *Chandra* and *XMM-Newton* to determine its precise spin-down rate. With a period derivative of $\dot{P} = 1.265 \times 10^{-13}$, PSR J1813–1749 is the third most energetic pulsar in the Galaxy, having spin-down luminosity $\dot{E} = 5.6 \times 10^{37}$ erg s^{–1}. Lack of pulsed detection in a deep radio search from the Green Bank Telescope, and in γ -rays from *Fermi*, are reported. We reconsider the distance to PSR J1813–1749/G12.82–0.02 in view of its large X-ray measured column density, $N_{\text{H}} = 10 \times 10^{22}$ cm^{–2}, which exceeds the visual extinction $A_V = 9.1$ to a young stellar cluster at $d = 4.8$ kpc that has been associated with it. Although the distance may well be larger, existing data do not constrain it further. The small radiative output of PSR J1813–1749/G12.82–0.02 in all bands would not exceed its spin-down power at any distance in the Galactic disk.

Subject headings: ISM: individual objects (HESS J1813–178, G12.82–0.02) — ISM: supernova remnants — pulsars: individual (PSR J1813–1749)

1. INTRODUCTION

HESS J1813–178 is one of the brightest and most compact TeV sources discovered in the HESS Galactic Plane Survey (Aharonian et al. 2005, 2006). It coincides with the young shell-type radio supernova remnant (SNR) G12.82–0.02 and the 2–10 keV X-ray source AX J1813–178 (Brogan et al. 2005). It is also detected in 20–100 keV X-rays as the *INTEGRAL* source IGR J18135–1751 (Ubertini et al. 2005). High-resolution X-ray studies resolved the X-ray emission into a point source and bright surrounding nebula (Funk et al. 2007; Helfand et al. 2007), whose properties indicate that a young, energetic rotation-powered pulsar is responsible for the extended X-rays, and probably the TeV radiation as well. A nearby young stellar cluster Cl 1813–178 at a kinematic distance of 4.8 kpc was discovered by Messineo et al. (2008, 2011), who suggested this as a possible birth place of the pulsar progenitor.

We discovered 44.7 ms X-ray pulsations from the point source in an *XMM-Newton* observation (Gotthelf & Halpern 2009). A 2.5σ detection of spin-down was also indicated in the long (98 ks) observation, suggesting that PSR J1813–1749 is one of the most energetic pulsars. In order to confirm and refine the high spin-down rate, we obtained two new X-ray observations, the results of which we report in this Letter.

2. X-RAY PULSAR OBSERVATIONS

A summary of the observations and results used here is given in Table 1. After the initial pulsar discovery on 2009 March 27, PSR J1813–1749 was observed a second time by *XMM-Newton* using the European Photon Imaging Camera (EPIC; Turner et al. 2003). The EPIC pn CCD was operated in small-window mode ($4'3 \times 4'3$ field of view; 29% dead time). This mode provides 5.7 ms time resolution. Data were also acquired with the two EPIC MOS CCD cameras (MOS1 and MOS2). These were operated in full frame mode with a time resolution of 2.6 s, insufficient for pulsar timing, and are not used

here. In order to optimize the signal and minimize contamination from the pulsar wind nebula (PWN), photons were extracted in the 2–10 keV band from a radius of $20''$ around the pulsar position.

An observation was also obtained using the *Chandra* Advanced Camera for Imaging and Spectroscopy (ACIS) operated in continuous-clocking (CC) mode to provide a time resolution of 2.85 ms. To achieve the fast timing in CC mode, one spatial dimension of the CCD image (the row number) is lost. To minimize contamination from the PWN, five columns were extracted around the pulsar position. Although background was estimated from nearby regions in both the *XMM-Newton* and *Chandra* images, it is difficult to subtract the background accurately because of the structured PWN surrounding the pulsar.

The photons arrival times were transformed to the solar system barycenter in Barycentric Dynamical Time (TDB) using the *Chandra* measured coordinates given in Helfand et al. (2007) and listed in Table 2. The best fitted period was determined for each data set using the Z_1^2 (Rayleigh) test (Strutt 1880; Buccheri et al. 1983). After determining the period derivative accurately over the 3 yr span of the observations, the individual observations were analyzed again using Z_1^2 , this time with \dot{P} held as a fixed parameter. The best periods so determined are shown in Figure 1 and Table 1, and the final $\dot{P} = 1.26545(64) \times 10^{-13}$ is given in Table 2. This is $< 1\sigma$ from the originally estimated value in Gotthelf & Halpern (2009).

Figure 2 shows the individual folded light curves of PSR J1813–1749 from the three observations, with background subtracted and the counts per bin normalized to 1. Because the incoherent timing solution fits only for frequency, not phase, the pulse profiles were aligned arbitrarily. The pulsed fraction is $\approx 50\%$. The *Chandra* light curve provides a better estimate of the pulsed fraction because it is possible to extract background closer to the pulsar than it is in the *XMM-Newton* image.

TABLE 1
TIMING OBSERVATIONS OF PSR J1813–1749

Mission	Instrument/Mode	ObsID	Date (UT)	Mid-Date (MJD)	Exp. (s)	Frequency (Hz)
<i>XMM-Newton</i>	EPIC pn SW	0552790101	2009 Mar 27–28	54,918.14	98,360	22.37171236(27)
<i>XMM-Newton</i>	EPIC pn SW	0650310101	2011 Mar 13	55,633.86	21,849	22.3677988(33)
<i>Chandra</i>	ACIS-S3 CC	12549	2012 Feb 12	55,969.24	20,077	22.3659583(35)

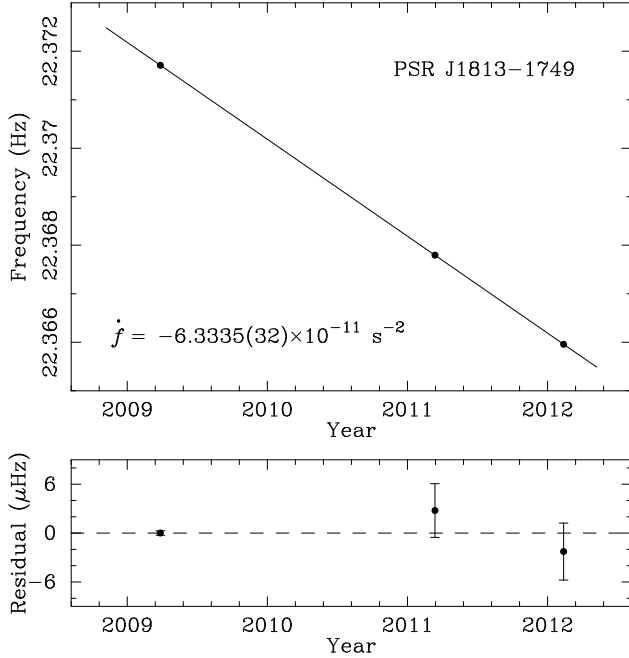


FIG. 1.— χ^2 fit to the measured frequencies of PSR J1813–1749. The bottom panel shows the residuals from the fit.

The derived physical parameters in the magnetic dipole model are spin-down power $\dot{E} \equiv 4\pi^2 I \dot{P} P^{-3} = 5.6 \times 10^{37} \text{ erg s}^{-1}$, surface dipole magnetic field strength $B_s \equiv 3.2 \times 10^{19} (P \dot{P})^{1/2} = 2.4 \times 10^{12} \text{ G}$, and characteristic age $\tau_c \equiv P/2\dot{P} = 5600 \text{ yr}$.

3. SEARCH FOR GAMMA-RAY PULSATIONS

Although a possible association of the *Fermi* source 0FGL J1814.3–1739 with HESS J1813–178 was noted by Abdo et al. (2009), the 2FGL catalog (Nolan et al. 2012) indicates only a confused source 2FGL J1814.1–1735c with a 95% error radius of $4'8$ that lies $16'6$ from HESS J1813–178. Marelli et al. (2011) derived a flux upper limit of $< 3 \times 10^{-11} \text{ erg cm}^{-2} \text{ s}^{-1}$ ($> 100 \text{ MeV}$) from *Fermi* data at the position of PSR J1813–1749. The *Fermi* luminosity limit (assumed isotropic) in Table 3 is not inconsistent with the trend and scatter among efficiencies of γ -ray pulsars as seen in Figure 6 of Abdo et al. (2010a) or Figure 2 of Marelli et al. (2011), although it is below the best fit of the high \dot{E} population. The *Fermi* upper limit lies above an extrapolation of the HESS spectrum, so the *Fermi* data are not sensitive enough to constrain the γ -ray emission mechanism.

For completeness, we have searched the *Fermi* data at the position of PSR J1813–1749 for pulsations using the X-ray measured timing parameters and their errors in Table 2 to restrict the parameters of the search. To match the time span of the X-ray observations, we ex-

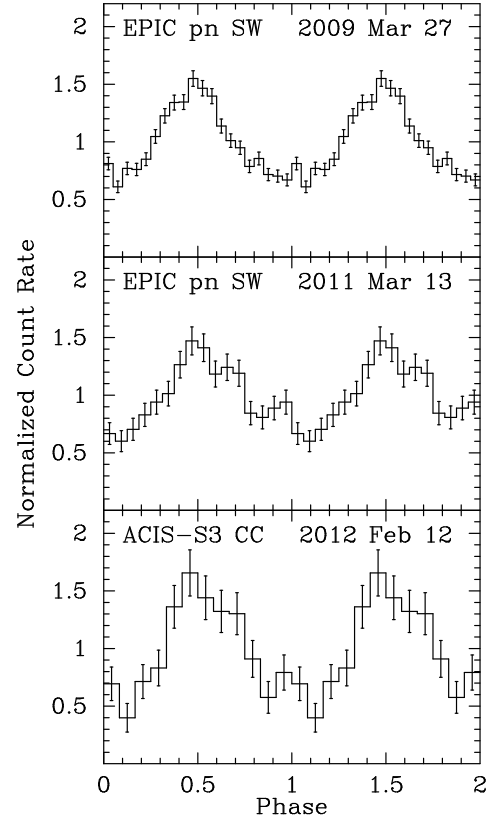


FIG. 2.— Pulse profiles of PSR J1813–1749 in the 2–10 keV band, folded according to the timing parameters in Tables 1 and 2. Background from nearby regions of the PWN has been subtracted, although it is not possible to do this exactly. The pulsed fraction is $\approx 50\%$. The pulses have been aligned arbitrarily in phase.

tracted LAT data from 2009 March 27 to 2012 February 12. These data were reprocessed using the “Pass 7” event reconstruction algorithm. We selected only class 2 “diffuse” photons for zenith angles $< 100^\circ$ and restricted the energy range to $> 500 \text{ MeV}$ to minimize solar limb and diffuse Galactic γ -ray background contamination. The photon arrival times were corrected to the solar system barycenter. For our nominal pulsar search we extracted photons from a 1.5° radius aperture.

Because the sparse X-ray observations do not yield a phase-connected ephemeris, unknown timing noise could limit the time span of a coherent pulsar search. Accordingly, we grouped the photons into intervals of 10 days and performed a Z_5^2 test (summed over five harmonics) to allow for a complex profile with narrow features. For each time interval, we searched a range of f, \dot{f} centered on interpolated values at the test epoch using the timing parameters in Table 2. The search range corresponds to three times the 1σ uncertainty in each of f and \dot{f} . We oversampled in each of these parameters by a factor of

TABLE 2
TIMING PARAMETERS FOR PSR J1813–1749

Parameter	Value
R.A. (J2000) ^a	18 ^h 13 ^m 35. ^s 166
Decl. (J2000) ^a	−17°49′57″48
Epoch (MJD)	54918.14
Period, P (s)	0.04469930526(54)
Period derivative, \dot{P}	$1.26545(64) \times 10^{-13}$
Frequency, f (Hz)	22.37171236(27)
Frequency derivative, \dot{f} (Hz s ^{−1})	$−6.3335(32) \times 10^{-11}$
Characteristic age, τ_c (yr)	5600
Spin-down luminosity, \dot{E} (erg s ^{−1})	5.6×10^{37}
Surface dipole magnetic field, B_s (G)	2.4×10^{12}

NOTE. — 1σ uncertainties are given.

^a *Chandra* ACIS-I position from Helfand et al. (2007).

three in the highest test harmonic to ensure sensitivity to sharp pulse profiles.

None of the 106 resulting searches yielded a significant signal above the noise. We also summed the power from these searches for each f, \dot{f} pair, increasing the signal sensitivity by a factor of ~ 10 . No significant signal was apparent. To explore a range of instrumental parameters that might be more sensitive, we repeated our search for extraction radii 1.0°, 1.5°, 2.0°, 2.5°, low-energy cutoff $E_{\min} = 100, 300, 500$ MeV, Z_n^2 harmonics $n = 1, 3, 5$, and time intervals 10, 30, 60, 120 days. We also used the H -test (de Jager et al. 1989); from a range of harmonics, this test selects the n that results in the most significant Z_n^2 value. Despite the expanded range of parameter space, no signal stronger than the expected noise is detected in each search.

4. RADIO PULSAR SEARCH

The location of PSR J1813–1749 was searched unsuccessfully for radio pulsations at the Parkes telescope in 2005, with a resulting limit on period-averaged flux density at 1.4 GHz of $S_{1.4} < 0.07$ mJy, assuming a 10% duty cycle (Helfand et al. 2007). In 2009 we did two, more sensitive observations at the NRAO Green Bank Telescope (GBT).

On 2009 May 25 we used the GUPPI spectrometer¹ to sample an 800 MHz band centered at 2 GHz, recording data from each of 512 frequency channels every 0.163 ms. The integration lasted for 1.8 hr. On 2009 August 17 we did a similar observation at the GBT, but with an integration time of 8.5 hr. We analyzed both data sets using standard pulsar search techniques implemented in PRESTO (Ransom 2001), but found no pulsar candidates. The data were searched in dispersion measure up to 3360 pc cm^{−3}, twice the total Galactic value predicted for this line of sight by the Cordes & Lazio (2002) electron distribution model.

The flux density limits for these observations at 2 GHz and for the period of the pulsar, assuming a 10% pulsar duty cycle, are 0.013 mJy and 0.006 mJy, respectively. Converting to 1.4 GHz, assuming a typical pulsar spectral index of -1.6 , these correspond to $S_{1.4} < 0.023$ mJy and $S_{1.4} < 0.01$ mJy, respectively. For an assumed distance of 4.8 kpc (see below), the luminosity limit of

our most sensitive radio search is $L_{1.4} \equiv S_{1.4}d^2 < 0.2$ mJy kpc². With one exception (Abdo et al. 2010b), all young pulsars with detected radio pulsations are more luminous than this (see Camilo et al. 2009a,b), which holds true even for a distance of 7 kpc.

A curious discovery of a time-variable point source in VLA 4.85 GHz data at the location of PSR J1813–1749 was reported by Dzib et al. (2010). The measured flux density of 0.18 ± 0.02 mJy in 2006 February was 1.9 ± 0.7 times larger than an upper limit obtained in 2009 March. We are not aware if the single detection has been duplicated. At 4.8 GHz, a typical rotation-powered radio pulsar is some seven times fainter than at 1.4 GHz. Our three flux density limits extrapolated to 4.8 GHz are thus a factor of approximately 20–120 times smaller than the time-variable compact source detection claimed by Dzib et al. (2010), which therefore almost certainly does not arise from pulsed emission².

5. DISCUSSION

5.1. Distance, Environment, and Associations

The total Galactic H I column in the direction of G12.82–0.02 is only $N_{\text{H}} = 1.9 \times 10^{22}$ cm^{−2} (Dickey & Lockman 1990) or 1.3×10^{22} cm^{−2} (Kalberla et al. 2005), while Brogan et al. (2005) find that the molecular column density between 0 and 4 kpc is $N(\text{H}_2) = 8 \times 10^{22}$ cm^{−2} by integrating the CO data of Dame et al. (2001). Higher resolution CO mapping by Funk et al. (2007) using NANTEN, with a beam size of 2.6 and a grid spacing of 4′, found $N(\text{H}_2) = 9 \times 10^{22}$ cm^{−2} at the position of G12.82–0.02. Thus, the total X-ray measured column density to G12.82–0.02 of $N_{\text{H}} = (10 \pm 1) \times 10^{22}$ cm^{−2} (Funk et al. 2007; Helfand et al. 2007) can be accounted for if G12.82–0.02 lies at a distance ≥ 4 kpc. From this, and the apparent free-free absorption of G12.82–0.02 by the W33 star-forming region at a distance of 4.3 kpc, previous authors (Brogan et al. 2005; Helfand et al. 2007; Gotthelf & Halpern 2009) have concluded that the distance to G12.82–0.02 is ≈ 4.5 kpc.

Messineo et al. (2008, 2011) discovered a young stellar cluster in Two Micron All Sky Survey infrared images on the edge of the W33 complex near G12.82–0.02. Dubbed Cl 1813–178, the cluster is centered 4.4 south-west of G12.82–0.02, most of its members falling within 3.5 of the cluster center. Messineo et al. (2011) concluded that it is one of several clusters belonging to the W33 complex. They derived a spectrophotometric distance to Cl 1813–178 of 3.6 ± 0.7 kpc, and a kinematic distance of 4.8 ± 0.3 kpc from the radial velocity ($v_{\text{LSR}} = +62 \pm 4$ km s^{−1}) of the brightest star in the cluster. Rich in massive, young stars, and containing a second SNR G12.72–0.00, this seems an ideal birth place for PSR J1813–1749. Messineo et al. (2011) determined an age of 4–4.5 Myr for the cluster, with a spread in age of 1 Myr based on the simultaneous presence of red supergiants, Wolf–Rayet, and Of stars. The total mass of the cluster is $\geq 10,000 M_{\odot}$. It is plausible that the progenitors of both G12.82–0.02 and G12.72–0.00 were born in the cluster, and had masses similar to the estimated

² Radio magnetars display both flat spectra and highly variable emission (e.g., Camilo et al. 2007), but PSR J1813–1749 is not a magnetar.

¹ <https://safe.nrao.edu/wiki/bin/view/CICADA/GUPPiUsersGuide>

TABLE 3
LUMINOSITY AND RADIATIVE EFFICIENCY OF PSR J1813–1749/G12.82–0.02

Mission	Energy Band	Source	Flux ^a (erg cm ⁻² s ⁻¹)	Luminosity ^b (erg s ⁻¹)	Efficiency	Flux Reference
<i>Chandra</i>	2–10 keV	AX J1813–178	7.2×10^{-12}	2.0×10^{34}	3.5×10^{-4}	Helfand et al. (2007)
<i>INTEGRAL</i>	20–100 keV	IGR J18135–1751	2.6×10^{-11}	7.0×10^{34}	1.3×10^{-3}	Bird et al. (2010)
<i>Fermi</i>	> 100 MeV	...	$< 3 \times 10^{-11}$	$< 8.3 \times 10^{34}$	$< 1.5 \times 10^{-3}$	Marelli et al. (2011)
HESS	> 200 GeV	HESS J1813–178	1.8×10^{-11}	4.9×10^{34}	8.8×10^{-4}	Aharonian et al. (2006)

^a Unabsorbed flux, including pulsar and PWN.

^b Luminosity assuming $d = 4.8$ kpc.

main-sequence turnoff, $25 - 35 M_{\odot}$. Only 13 such massive clusters are known in the Galaxy (Messineo et al. 2009).

However, evidence that may contradict an association of G12.82–0.02 with Cl 1813–178 are the discrepant absorption column densities to the two objects. The average visual extinction to Cl 1813–178 of $A_V = 9.1$ (Messineo et al. 2011), estimated from the infrared colors of 25 of its member stars, corresponds to an equivalent X-ray absorption of only $N_H = 1.6 \times 10^{22}$ cm⁻² according to the relation of Predehl & Schmitt (1995). The highest extinction for a cluster member is $A_V = 17$. Either of these extinction values do not account for the X-ray measured $N_H = (10 \pm 1) \times 10^{22}$ cm⁻² to G12.82–0.02. Although the difference may be made up by half of the molecular column of $N(\text{H}_2) = 9 \times 10^{22}$ cm⁻² measured by Funk et al. (2007), this would require nearly all of the X-ray measured column density to G12.82–0.02 to lie behind Cl 1813–178. This means that G12.82–0.02 is not constrained to be at the kinematic distance of Cl 1813–178. There is no evidence that the SNR is interacting physically with molecular gas that could be associated with it. In addition, it is likely that some of the molecular hydrogen on the line of sight, which has $v_{\text{LSR}} \leq +60$ km s⁻¹, is in the far branch of the double-valued radial velocity curve at 12–16 kpc. This means that G12.82–0.02 could be anywhere from 5–12 kpc distant, unconstrained by the distribution of molecular gas. If so, it could be expected to have H I absorption features up to $v_{\text{LSR}} \approx +170$ km s⁻¹, the tangent point velocity at $d = 8.3$ kpc. Brogan et al. (2005) report that no H I absorption features are seen toward G12.82–0.02 at $v_{\text{LSR}} \geq +55$ km s⁻¹ in data from the Southern Galactic Plane Survey, although the signal to noise is low; therefore, their absence is inconclusive.

Indirect evidence for a larger distance comes from a comparison with the absorption to the bright LMXB GX 13+1 that lies only 0.7° from G12.82–0.02 along the Galactic plane. The total Galactic H I column densities are substantially the same along these lines of sight. Converting the CO intensity of Dame et al. (2001) to H₂ column density, we find $N(\text{H}_2) = 5 \times 10^{22}$ cm⁻² in the direction of GX 13+1. The distance to GX 13+1 was estimated as 7 ± 1 kpc (Bandyopadhyay et al. 1999) from the IR spectroscopic classification (K5III) and reddening ($A_V = 13.2 - 17.6$) of its companion star, while its X-ray column density measured by ASCA is $N_H = (2.9 \pm 0.1) \times 10^{22}$ cm⁻² (Ueda et al. 2001). The X-ray measured absorption is consistent with being due mostly to molecular material. As this is less than one-third the X-ray measured N_H to G12.82–0.02, it suggests that the latter may be farther than 7 kpc.

Finally, we note that these comparisons involving individual stars are subject to the caveat that extinction and CO may be clumpy on small scales that are not resolved by the CO surveys. Lacking certainty, we therefore retain the previously adopted distance of 4.8 kpc to calculate the luminosities in Table 3. Even at a distance of 15 kpc, or a factor of 10 higher in luminosity than assumed in Table 3, the radiative efficiencies in all bands would be plausible for such an energetic pulsar. The *Fermi* upper limit would be consistent with the GeV luminosities of the bulk of the high \dot{E} pulsar population. The TeV luminosity would still be $< 1\%$ of \dot{E} , although PSR J1813–1749 would then have the highest luminosity TeV PWN in the Galaxy.

5.2. Age and Energetics

HESS J1813–178 is one of the more compact TeV sources to be associated with an SNR. The Gaussian extent of the source is only $\sigma = 2.2 \pm 0.4$ (Aharonian et al. 2006), while the radio shell of G12.82–0.02 is 2.5 in diameter (Brogan et al. 2005), corresponding to a radius of 1.7 pc at a distance of 4.8 kpc. The small size can be explained by a young age. Although the characteristic age of PSR J1813–1749 is 5600 yr, its true age may be significantly smaller than this if it were born with an initial period not much less than its present period. Brogan et al. (2005) estimate a free-expansion age for G12.82–0.02 of only $340 (d/4.8 \text{ kpc}) (v_s/5000 \text{ km s}^{-1})$ yr, which would be consistent with having swept up little interstellar matter at the assumed distance. Even if at $d = 20$ kpc, they note that the Sedov–Taylor age for an explosion energy of $E_0 = 10^{51}$ erg and an ambient density of 1 cm^{-3} is ≈ 2500 yr. Using the pulsar plus PWN fluxes, the ratio $L_x(2 - 10 \text{ keV})/L_{\gamma}(> 200 \text{ GeV})$ is ≈ 0.4 , which is typical for the \dot{E} and characteristic age of PSR J1813–1749 (Mattana et al. 2009).

A detailed model of the evolution and multiwavelength emission from HESS J1813–178 was constructed by Fang & Zhang (2010), including particle acceleration in both the PWN and SNR. They assumed $d = 4.7$ kpc, an underluminous explosion $E_0 = 0.5 \times 10^{50}$ erg, an ambient density of 1.4 cm^{-3} , and a present age of 1200 yr. At this stage the reverse shock has not yet reached the PWN, which has a radius of 0.7 pc. The results are that the PWN is responsible for the X-ray and the TeV emission, while the SNR shell is only detectable in radio. The TeV emission is inverse Compton scattered microwave background or IR photons from dust, while the stellar light is a small contributor. Energy densities for IR and starlight were taken to be $U_{\text{IR}} = 1.0 \text{ eV cm}^{-3}$

and $U_* = 1.5 \text{ eV cm}^{-3}$, respectively.

A justification for these energy densities was not given, but an assumed association with Cl 1813–178 is not consistent with such small values. The massive stars in the cluster are very luminous; the total of just the 25 young cluster members is $L_* = 1.04 \times 10^7 L_\odot$ at the kinematic distance of 4.8 kpc (Messineo et al. 2011). If G12.82–0.02 is at the projected distance of 4.4 ($r = 6.2 \text{ pc}$) from the cluster center, the energy density in its vicinity can be approximated as $U_* = L_*/4\pi r^2 c = 180 \text{ eV cm}^{-3}$. Even if this is reduced by a factor ~ 2 due to projection effects, it is still much larger than $U_{\text{IR}} + U_* = 2.5 \text{ eV cm}^{-3}$ assumed by Fang & Zhang (2010). This suggests that either their model should be revised to account for the energy density in starlight from Cl 1813–178, or more likely, G12.82–0.02/HESS J1813–178 lies at a larger distance than Cl 1813–178. If the distance is much larger, this would also allow a more energetic supernova explosion.

6. CONCLUSIONS

We obtained new X-ray timing observations of PSR J1813–1749, which precisely refine the previously suggested high spin-down rate. With $\dot{E} = 5.6 \times 10^{37} \text{ erg s}^{-1}$, PSR J1813–1749 is the third

most energetic pulsar in the Galaxy after the Crab and the recently discovered PSR J2022+3842 (Arzoumanian et al. 2011). Uncertainty about the distance to PSR J1813–1749/G12.82–0.02 arises from discrepant absorption column densities to an assumed host stellar cluster and another bright X-ray source along the line of sight. We conclude that the distance may be larger than the previously adopted 4.8 kpc, but it is difficult to quantify further. The small radiative efficiency of PSR J1813–1749/G12.82–0.02 in all bands allows any distance in the Galactic disk without exceeding its spin-down power. A more sensitive observation of 21 cm H I absorption against G12.82–0.02 is needed to pin down its distance. It would be worthwhile to construct models for the SNR evolution of G12.82–0.02 and the TeV emission from HESS J1813–178 for a larger distance.

We thank Roland Kothes for helpful discussions. This investigation is based on observations obtained with *XMM-Newton*, an ESA science mission with instruments and contributions directly funded by ESA Member States, and NASA. Support for this work was provided by NASA through *Chandra* award SAO G01-12075X issued by the Chandra X-ray Observatory Center, which is operated by the Smithsonian Astrophysical Observatory for and on behalf of NASA under contract NAS8-03060, and by *Fermi* guest investigator grant NNX11AO36G.

REFERENCES

- Abdo, A. A., Ackermann, M., Ajello, M., et al. 2009, *ApJS*, 183, 46
 Abdo, A. A., Ackermann, M., Ajello, M., et al. 2010a, *ApJS*, 187, 460
 Abdo, A. A., Ackermann, M., Ajello, M., et al. 2010b, *ApJ*, 711, 64
 Aharonian, F., Akhperjanian, A. G., Aye, K.-M., et al. 2005, *Science*, 307, 1938
 Aharonian, F., Akhperjanian, A. G., Bazer-Bachi, A. R., et al. 2006, *ApJ*, 636, 777
 Arzoumanian, Z., Gotthelf, E. V., Ransom, S. M., et al. 2011, *ApJ*, 739, 39
 Bandyopadhyay, R. M., Shahbaz, T., Charles, P. A., & Naylor, T. 1999, *MNRAS*, 306, 417
 Bird, A. J., Bazzano, A., Bassani, L., et al. 2010, *ApJS*, 186, 1
 Brogan, C. L., Gaensler, B. M., Gelfand, J. D. et al. 2005, *ApJ*, 629, L105
 Buccheri, R., Bennett, K., Bignami, G. F., et al. 1983, *A&A*, 128, 245
 Camilo, F., Ng, C.-Y., Gaensler, B. M., et al. 2009a, *ApJ*, 703, L55
 Camilo, F., Ransom, S. M., Peñalver, J., et al. 2007, *ApJ*, 669, 561
 Camilo, F., Ray, P. S., Ransom, S. M., et al. 2009b, *ApJ*, 705, 1
 Cordes, J. M., & Lazio, T. J. W. 2002, *arXiv:astro-ph/0207156*
 Dame, T. M., Hartmann, D., & Thaddeus, P. 2001, *ApJ*, 547, 792
 de Jager, O. C., Raubenheimer, B. C., & Swanepoel, J. W. H. 1989, *A&A*, 221, 180
 Dickey, J. M., & Lockman, F. J. 1990, *ARA&A*, 28, 215
 Dzib, S., Rodríguez, L. F., & Loinard, L. 2010, *RevMexAA*, 46, 153
 Fang, J., & Zhang, L. 2010, *ApJ*, 718, 467
 Funk, S., Hinton, J. A., Moriguchi, Y., et al. 2007, *A&A*, 470, 249
 Gotthelf, E. V., & Halpern, J. P. 2009, *ApJ*, 700, L158
 Helfand, D. J., Gotthelf, E. V., Halpern, J. P., et al. 2007, *ApJ*, 665, 1297
 Kalberla, P. M. W., Burton, W. B., Hartmann, D., et al. 2005, *A&A*, 440, 775
 Marelli, M., De Luca, A., & Caraveo, P. A. 2011, *ApJ*, 733, 82
 Mattana, F., Falanga, M., Götz, D., et al. 2009, *ApJ*, 694, 12
 Messineo, M., Davies, B., Figer, D. F., et al. 2011, *ApJ*, 733, 41
 Messineo, M., Davies, B., Ivanov, V. D., et al. 2009, *ApJ*, 697, 701
 Messineo, M., Figer, D. F., Davies, B., et al. 2008, *ApJ*, 683, L155
 Nolan, P. L., Abdo, A. A., Ackermann, M., et al. 2012, *ApJS*, 199, 31
 Predehl, P., & Schmitt, J. H. M. M. 1995, *A&A*, 293, 889
 Ransom, S. M. 2001, PhD thesis, Harvard Univ
 Strutt, J. W. 1880, *Philos. Mag.*, 10, 73
 Turner, M. J. L., Briel, U. G., Ferrando, P., Griffiths, R. G., & Villa, G. E. 2003, *Proc. SPIE*, 4851, 169
 Ubertini, P., Bassani, L., Malizia, A., et al. 2005, *ApJ*, 629, L109
 Ueda, Y., Asai, K., Yamaoka, K., Dotani, T., & Inoue, H. 2001, *ApJ*, 556, L87